

See discussions, stats, and author profiles for this publication at: <https://www.researchgate.net/publication/231659625>

# Quantitative Spectroscopic Studies of the Photoexcited State Properties of Methano- and Pyrrolidino-[60]fullerene Derivatives

ARTICLE *in* THE JOURNAL OF PHYSICAL CHEMISTRY C · JULY 1997

Impact Factor: 4.77 · DOI: 10.1021/jp971067k

---

CITATIONS

51

---

READS

19

5 AUTHORS, INCLUDING:



Bin ma

Lanzhou University

204 PUBLICATIONS 6,277 CITATIONS

SEE PROFILE



Xian-Fu Zhang

Institute of applied photochemistry, Hebei Pr...

76 PUBLICATIONS 715 CITATIONS

SEE PROFILE

# Quantitative Spectroscopic Studies of the Photoexcited State Properties of Methano- and Pyrrolidino-[60]fullerene Derivatives

Bin Ma, Christopher E. Bunker, Radhakishan Guduru, Xian-Fu Zhang, and Ya-Ping Sun\*

Department of Chemistry, Howard L. Hunter Chemistry Laboratory, Clemson University,  
Clemson, South Carolina 29634-1905

Received: March 25, 1997; In Final Form: May 30, 1997<sup>®</sup>

UV/vis absorption and fluorescence spectra and fluorescence quantum yields and lifetimes of a series of methano- and pyrrolidino-[60]fullerene derivatives in different solvents are studied systematically. The absorption and fluorescence properties of the derivatives with different substituents are somewhat different from those of [60]fullerene, but very similar among themselves, indicating that the low-lying transitions and the photoexcited state processes are dictated by the electronic structures of functionalized [60]fullerene cages. The results also allow an examination of the issue concerning discrepancies between experimentally determined transition probabilities and those calculated in terms of the Strickler–Berg equation for fullerene molecules. In addition, quenchings of the excited singlet states of the [60]fullerene derivatives by electron donor *N,N*-diethylaniline (DEA) and the formation of emissive fullerene–DEA exciplexes in solvents of different polarities are investigated.

## Introduction

The electronic absorption and emission properties of fullerenes, especially [60]fullerene ( $C_{60}$ ) and [70]fullerene ( $C_{70}$ ), have attracted much attention.<sup>1</sup> Because of the high degree of symmetry in the closed-shell electronic configuration, the low-lying electronic transitions in  $C_{60}$  are only weakly allowed. The observed  $C_{60}$  absorption band in the visible is very weak, with the molar absorptivity at the band maximum of only  $\sim 950 \text{ M}^{-1} \text{ cm}^{-1}$ .<sup>2–4</sup> For  $C_{70}$ , the symmetry-related forbidden selection is somewhat relaxed, and transition probabilities of low-lying excited states become much higher ( $\sim 21\,000 \text{ M}^{-1} \text{ cm}^{-1}$  at  $\sim 470 \text{ nm}$ , the maximum of a broad absorption band in the visible).<sup>5,6</sup> The fullerenes are only weakly fluorescent, regardless of experimental conditions.<sup>3–8</sup> The low fluorescence yields ( $3.2 \times 10^{-4}$  for  $C_{60}$  and  $5.7 \times 10^{-4}$  for  $C_{70}$  in room-temperature toluene)<sup>8</sup> are not only due to rapid intersystem crossing to the formation of excited triplet states but also attributable to small fluorescence radiative rate constants as a result of weak electronic transitions.

Methano- $C_{60}$  and pyrrolidino- $C_{60}$  derivatives represent two important classes of functionalized fullerene compounds.<sup>9–12</sup> They are investigated for potential technological applications. For example, methano- $C_{60}$  derivatives are being considered as inhibitors for the protease of the HIV virus<sup>13,14</sup> and as efficient photosensitizers in the generation of singlet molecular oxygen for photodynamic activities.<sup>15</sup> The fullerene derivatives are also being examined for their nonlinear optical properties.<sup>16,17</sup> Similar to the parent  $C_{60}$ , the methano- $C_{60}$  and pyrrolidino- $C_{60}$  derivatives are excellent nonlinear absorbers, and their more favorable solubility properties are advantageous in the fabrication of optical limiting devices. Apparently, many of the potential technological applications under consideration for the  $C_{60}$  derivatives are related to their photoexcited states, for which systematic investigations are still in demand.<sup>18,19</sup> In addition, since methano- $C_{60}$  and pyrrolidino- $C_{60}$  derivatives are structurally perturbed fullerene molecules, the similarities and differences in their photophysical behavior in comparison with the parent  $C_{60}$  may provide a more general understanding of the

electronic structures and excited state properties of fullerenes. In this paper, we report a systematic spectroscopic study of seven  $C_{60}$  derivatives in room-temperature solution. Absorption properties of the derivatives were examined in detail in different solvents. Fluorescence spectra and quantum yields were obtained on a near-infrared-sensitive emission spectrometer (up to 1200 nm), and fluorescence lifetimes were determined using the time-correlated single-photon-counting technique. The absorption and emission properties of the different  $C_{60}$  derivatives are quite similar among themselves, but somewhat different from those of  $C_{60}$ . With the photophysical results of the  $C_{60}$  derivatives, the issue concerning discrepancies between experimental fluorescence radiative rate constants and those calculated in terms of the Strickler–Berg equation<sup>20</sup> for fullerene molecules<sup>4,6,21,22</sup> becomes clearer. In addition, quenchings of the excited singlet states of  $C_{60}$  and the  $C_{60}$  derivatives by electron donor *N,N*-diethylaniline and the formation and solvent dependence of exciplexes are compared and discussed.

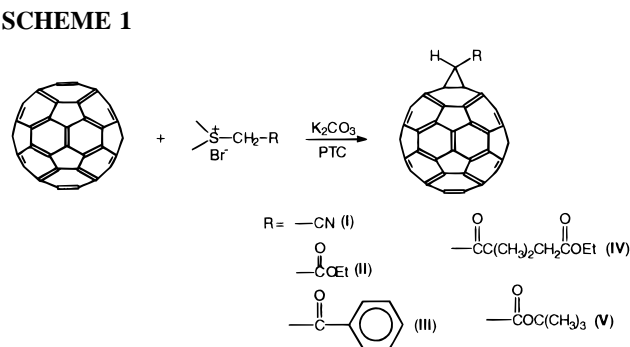
## Experimental Section

**Materials.**  $C_{60}$  (purity >99.5%) was obtained from Southern Chemical Group. The sample purity was checked by UV/vis absorption,  $^{13}\text{C}$  NMR, and matrix-assisted laser desorption ionization time-of-flight MS methods, and the sample was used without further purification. *N,N*-Diethylaniline (99%) was obtained from Aldrich and purified through reduced-pressure distillation before use. Hexane, toluene, *o*-xylene, dichloromethane, chloroform, acetonitrile, acetone, carbon disulfide, and *o*-dichlorobenzene (all spectrophotometric grade) were obtained from Burdick & Jackson, and 1,2,3,5-tetramethylbenzene (85% and the remaining fractions being other isomers) and 1,2,4-trimethylbenzene (98%) were obtained from Aldrich. The solvents were used as received because there was no interference of possible impurities in the wavelength range of interest according to absorption and emission spectroscopic measurements of the solvents. Rhodamine 101 (99%) was obtained from Fisher Scientific and used as a fluorescence standard.

**Methano- $C_{60}$  Derivatives I–V.** Methano- $C_{60}$  derivatives I–V were prepared by use of the reactions of  $C_{60}$  with stabilized

<sup>®</sup> Abstract published in *Advance ACS Abstracts*, July 1, 1997.

## SCHEME 1



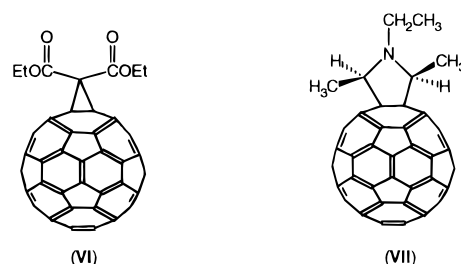
sulfonium ylides with cyano, carboxy, and carbonyl groups.<sup>23</sup> The one-pot preparation was carried out under phase transfer conditions. A toluene solution of  $\text{C}_{60}$ , sulfonium salt,  $\text{K}_2\text{CO}_3$ , and the phase transfer catalyst tetrabutylammonium bromide (TBAB) was mixed and reacted at room temperature. The stabilized sulfonium ylide generated *in situ* due to the deprotonation of the sulfonium salt by  $\text{K}_2\text{CO}_3$  under the catalysis of TBAB undergoes nucleophilic addition to  $\text{C}_{60}$ , followed by intramolecular substitution to form a methano- $\text{C}_{60}$  derivative with the simultaneous elimination of dimethyl sulfide (Scheme 1).

In a typical one-pot reaction, 100 mg (0.14 mmol) of  $\text{C}_{60}$  in 60 mL of anhydrous toluene, 0.16 mmol sulfonium bromide, 200 mg (1.45 mmol) of anhydrous  $\text{K}_2\text{CO}_3$ , and 20 mg (0.076 mmol) of the catalyst TBAB were added to a 100 mL round bottom flask. After purging with dry nitrogen gas, the flask was sealed and the reaction mixture was stirred at room temperature for 24 h. The mixture was then filtered to remove any solids and concentrated by evaporation under vacuum. Results from the matrix-assisted laser desorption ionization time-of-flight MS analysis show the presence of mono-, bis-, and tris-adducts. The mono-adduct was obtained after separation from higher order adducts through silica gel column chromatography using  $\text{CS}_2$  as an eluent. The methano- $\text{C}_{60}$  derivatives are brown solids and more soluble than  $\text{C}_{60}$  in common organic solvents such as chloroform. The yields for preparations of the methano- $\text{C}_{60}$  derivatives **I–V** are in the range 45–60%. Proton and  $^{13}\text{C}$  NMR results clearly demonstrate that the methylene bridge is at the [6,6]-ring junction. In contrast to the preparation of methano- $\text{C}_{60}$  derivatives based on addition reactions of diazo compounds,<sup>9,11,12,27</sup> no isomers having the “open” [6,5]-ring bridged form were found in the reaction mixtures of the sulfonium ylide addition.

**Methano- $\text{C}_{60}$  Derivative VI.** The methano- $\text{C}_{60}$  derivative **VI** was prepared following a procedure reported in the literature,<sup>24</sup> except that a lower molar ratio of bromomalonate to  $\text{C}_{60}$  (1.2:1) was used to promote the formation of mono-adduct. In the reaction, nucleophilic addition of a bromomalonate carbanion from the deprotonation of bromomalonate with sodium hydride was followed by an intramolecular substitution. The reaction mixture consists of mono-, bis-, and tris-adducts. The mono-adduct was separated from the mixture in 55% yield through silica gel column chromatography using toluene as eluent and was positively identified in matrix-assisted laser desorption ionization time-of-flight MS, proton and  $^{13}\text{C}$  NMR, and FT-IR characterizations.

**Pyrrolidino- $\text{C}_{60}$  Derivative VII.** The pyrrolidino- $\text{C}_{60}$  derivative **VII** was obtained from photochemical reactions of  $\text{C}_{60}$  and triethylamine in room-temperature toluene. The purification and structural characterization of the compound have been reported elsewhere.<sup>25</sup>

**Measurements.** Absorption spectra were obtained using a computer-controlled Shimadzu UV2101-PC spectrophotometer.



Emission spectra were recorded on a Spex Fluorolog-2 photon-counting emission spectrometer equipped with a 450 W xenon source, a Spex 340S dual-grating and dual-exit emission monochromator, and two detectors. The two gratings are blazed at 500 nm (1200 grooves/mm) and 1000 nm (600 grooves/mm). The room-temperature detector consists of a Hamamatsu R928P photomultiplier tube operated at  $-950$  V, and the thermoelectronically cooled detector consists of a near-infrared-sensitive Hamamatsu R5108 photomultiplier tube operated at  $-1500$  V. In fluorescence measurements, a Schott 540 nm (GG-540) or 610 nm (RG-610) color glass sharp-cut filter was placed before the emission monochromator to eliminate the excitation scattering. Minor distortion at the blue onset of the observed fluorescence spectra due to the filter was corrected by use of the transmittance profile of the filter. The slit of the excitation monochromator was 5 mm (19 nm resolution). For the emission monochromator, a wide slit of 5 mm (19 nm resolution) was used in fluorescence quantum yield measurements to reduce experimental uncertainties, and a narrow slit of 0.5 mm (2 nm resolution) was used in fluorescence spectral measurements to retain structures of the spectra. Unless specified otherwise, fluorescence spectra were corrected for nonlinear instrumental response by use of predetermined correction factors. The correction factors for the emission spectrometer were carefully determined by using a calibrated radiation standard from Optronic Laboratories.

Fluorescence decays were measured by using the time-correlated single-photon-counting (TCSPC) method. One TCSPC setup consists of a nitrogen flash lamp obtained from Edinburgh Instruments as excitation source. The flash lamp was operated at 50 kHz, and the wavelength of 317 nm was isolated using a band-pass filter with a 10 nm fwhm. Fluorescence decays were monitored through a 545 nm color glass sharp-cut filter. The detector consists of a Philips X2020 photomultiplier tube in a thermoelectronically cooled housing from the Products for Research, Inc. The photomultiplier tube was operated at  $-2$  kV using an EG&G 556 high-voltage power supply. The detector electronics from EG&G include two 9307 discriminators, a 457 biased time-to-amplitude converter, and a 916A multichannel analyzer. The instrument response function of the setup has a fwhm of  $\sim 2.0$  ns. The second TCSPC setup with an instrument response function of  $\sim 60$  ps (fwhm) has been described in detail elsewhere.<sup>26</sup> Fluorescence lifetimes were determined from observed decay curves and instrument response functions by use of the Marquardt nonlinear least-squares method.

## Results

**UV/Vis Absorption.** UV/vis absorption spectra of the methano- $\text{C}_{60}$  derivatives **I–VI** in room-temperature (22 °C) toluene are shown in Figure 1. The spectra are rather similar among themselves, but different from that of  $\text{C}_{60}$ .<sup>9,18,19,23</sup> Characteristic features in the spectra of the methano- $\text{C}_{60}$  derivatives include a small peak at  $\sim 700$  nm with molar absorptivities ranging from 200 to  $300 \text{ M}^{-1} \text{ cm}^{-1}$  and a sharp

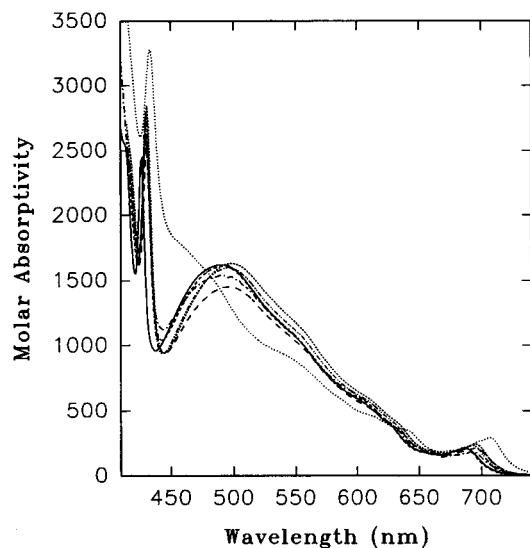


**Figure 1.** Absorption spectra of methano- $C_{60}$  derivatives **I** (---), **II** (---), **III** (---), **IV** (---), **V** (---), and **VI** (---) and pyrrolidino- $C_{60}$  derivative **VII** (···) in room-temperature toluene.

band in the 420–430 nm region.<sup>27</sup> The absorption spectrum of the pyrrolidino- $C_{60}$  derivative **VII** has the same features, but still somewhat different from the spectra of the methano- $C_{60}$  derivatives such that the latter have a maximum at  $\sim 500$  nm (Figure 1). Overall, the derivatives are stronger absorbers than  $C_{60}$ . The absorption spectral parameters in toluene are summarized in Table 1.

Absorption spectra of the  $C_{60}$  derivatives remain essentially the same in solvents of different polarities, for example, toluene vs methylene chloride or *o*-dichlorobenzene. In saturated hydrocarbon solvents such as hexane and methylcyclohexane, observed UV/vis absorption spectra of the  $C_{60}$  derivatives are slightly better resolved, with more detailed vibronic structures in the band at  $\sim 700$  nm (Figure 2). However, similar to  $C_{60}$ , the  $C_{60}$  derivatives have significantly different UV/vis absorption spectra in the solvent series of benzenes with different numbers of methyl substituents.<sup>8,28</sup> For example, observed UV/vis absorption spectra of **II** in toluene, *o*-xylene, 1,2,4-trimethylbenzene, and 1,2,3,5-tetramethylbenzene change in a characteristic fashion. As shown in Figure 3, the band at  $\sim 430$  nm progressively shifts to the red with solvents from toluene to 1,2,3,5-tetramethylbenzene, while there are essentially no changes in the longer wavelength portion of the spectra at all.

**Fluorescence Spectra.** Fluorescence spectra of the methano- and pyrrolidino- $C_{60}$  derivatives in room-temperature toluene are shown in Figure 2. The spectra are also very similar among themselves, but different from the fluorescence spectrum of  $C_{60}$ . The vibronic structures in the spectra are broad and are not affected by increasing the resolution of the spectrometer with narrower emission slits. Fluorescence spectra of the  $C_{60}$  derivatives are excitation wavelength independent and are only marginally affected by solvent changes, even in the solvent series of methyl-substituted benzenes (Figure 3). In saturated hydrocarbon solvents such as hexane and methylcyclohexane, observed fluorescence spectra are slightly better resolved (Figure 2). The fluorescence spectral parameters are also summarized in Table 1.

**Fluorescence Quantum Yields.** Fluorescence quantum yields of the  $C_{60}$  derivatives in room-temperature toluene were determined carefully in reference to the yield of  $C_{60}$  ( $3.2 \times 10^{-4}$ ), which was obtained using rhodamine 101 in ethanol as a fluorescence standard ( $\Phi_F = 1.0$ ).<sup>8,29</sup> As summarized in Table 2, fluorescence yields of the derivatives range from  $9.3 \times 10^{-4}$

to  $1.2 \times 10^{-3}$ , larger than that of  $C_{60}$ . Observed fluorescence quantum yields of the derivatives are also independent of excitation wavelengths. For the pyrrolidino- $C_{60}$  derivative **VII**, fluorescence quantum yields were also determined in several solvents of different polarities. The results were corrected for effects due to changes in solvent refractive index  $n$ .

$$\Phi_F = \Phi'_F (n/n_{SD})^{-2} \quad (1)$$

where SD represents the solvent for the standard from which the uncorrected fluorescence yield value  $\Phi'_F$  is obtained. The results show that the yields are only marginally solvent dependent (Table 2).

**Fluorescence Lifetimes.** Fluorescence decays of  $C_{60}$  and the  $C_{60}$  derivatives in room-temperature toluene or chloroform were measured using the time-correlated single-photon-counting method. For example, the fluorescence decay of the derivative **I** is shown in Figure 4. The decay curves can be deconvoluted well from corresponding instrumental response functions using a monoexponential equation.<sup>30</sup> The  $C_{60}$  fluorescence lifetime of 1.2 ns thus obtained in room-temperature toluene is in excellent agreement with the literature values.<sup>22,31</sup> Fluorescence lifetimes of the  $C_{60}$  derivatives are somewhat longer,  $\sim 1.5$  ns, and the results of different derivatives are again very similar (Table 2).

**Transition Probabilities and Radiative Rate Constants.** Fluorescence radiative rate constants of the  $C_{60}$  derivatives can be calculated from experimentally determined fluorescence quantum yields  $\Phi_F$  and lifetimes  $\tau_F$

$$k_{F,e} = \Phi_F / \tau_F \quad (2)$$

where the subscript e identifies experimentally determined fluorescence radiative rate constants. Results of  $C_{60}$  and the  $C_{60}$  derivatives are summarized in Table 2. For comparison, the radiative rate constants may be calculated, independent of the fluorescence quantum yield and lifetime results, in terms of electronic transition probabilities by use of the Strickler–Berg equation.<sup>20</sup>

$$k_{F,c} = 2.880 \times 10^{-9} n^2 \langle \nu_F^{-3} \rangle_{AV}^{-1} (g_0/g_e) \int (\epsilon/\nu) d\nu \quad (3)$$

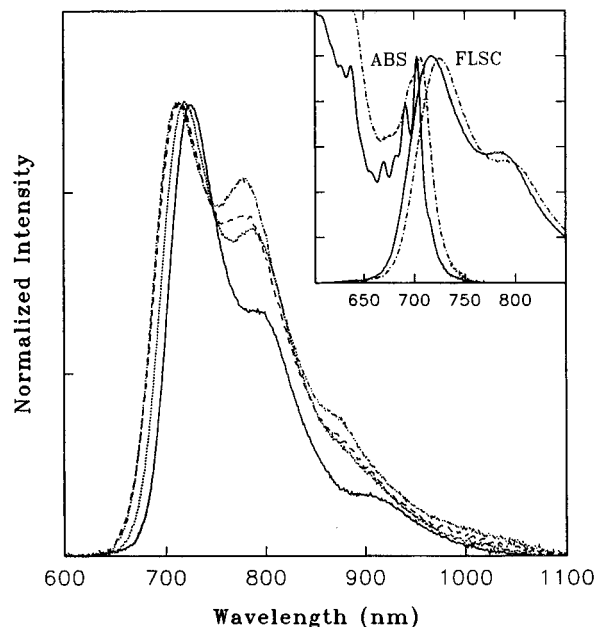
where the subscript c identifies calculated fluorescence radiative rate constants,  $g$  denotes state degeneracies,  $\epsilon$  represents molar absorptivities, and  $n$  is the refractive index of the solvent.

$$\langle \nu_F^{-3} \rangle_{AV}^{-1} = [\int I_F(\nu) d\nu] / [\int \nu^{-3} I_F(\nu) d\nu] \quad (4)$$

where  $I_F$  represents fluorescence intensities. While the calculation of the  $\langle \nu_F^{-3} \rangle_{AV}^{-1}$  term using observed fluorescence spectra is straightforward, the determination of the integration  $\int (\epsilon/\nu) d\nu$  from observed absorption spectra is somewhat more difficult. For  $C_{60}$ , it is known<sup>8,21,22</sup> that the inclusion of the entire long-wavelength absorption band (440–700 nm) significantly overestimates the electronic transition probabilities because the band is likely contributed by several low-lying electronic transitions. Similarly, the electronic transition probabilities of the  $C_{60}$  derivatives cannot be calculated by using the entire absorption bands in the visible. Instead, the  $\int (\epsilon/\nu) d\nu$  term due to the lowest excited singlet state was calculated by assuming a mirror image relationship between the absorption and fluorescence spectra. For example, the assumed relationship for the derivative **IV** is illustrated in Figure 5. The calculated fluorescence radiative rate constants of the  $C_{60}$  derivatives obtained with the assumption of a mirror image relationship between fluorescence and absorption bands and  $g_0 = g_e = 1$  are also summarized in Table 2.

TABLE 1: Absorption and Fluorescence Spectral Parameters of the C<sub>60</sub> Derivatives<sup>a</sup>

derivative	absorption bands (nm)	fluorescence bands (nm)
I	687, 615(sh), 555(sh), 491, 430	711, 777, 880(sh)
II	694, 617(sh), 560(sh), 498, 430	718, 785, 880(sh)
III	695, 620(sh), 554(sh), 499, 431	720, 789, 883(sh)
IV	696, 620(sh), 555(sh), 496, 431	719, 789, 892(sh)
V	695, 615(sh), 555(sh), 489, 430	716, 786, 880(sh)
VI	688, 615(sh), 551(sh), 491, 427	715, 778, 914(sh)
VII	707, 642(sh), 615(sh), 552, 480(sh), 434	726, 798, 912(sh)

<sup>a</sup> In room-temperature toluene, except for VI in chloroform.

**Figure 2.** Fluorescence spectra of the methano-C<sub>60</sub> derivatives IV (···, very similar for II and III, not shown), V (---), and VI (— · —, very similar for I, not shown) and the pyrrolidino-C<sub>60</sub> derivative VII (—) in room-temperature toluene ( $6 \times 10^{-5}$  M). Shown in the inset is a comparison of the absorption and fluorescence spectra of methano-C<sub>60</sub> derivative VII in hexane (—) and toluene (— · —).

**Electron Transfer Quenching and Exciplex Formation.** Similar to C<sub>60</sub>,<sup>1b,7a,32,33</sup> the methano-C<sub>60</sub> derivatives undergo electron transfer interactions with electron donor *N,N*-diethylaniline (DEA) in both ground and excited singlet states. The formation of ground state charge transfer complexes requires high DEA concentrations. At low DEA concentrations ( $<0.3$  M), the electron transfer quenching of excited singlet states and the formation of fullerene–DEA exciplexes may be studied without the interference of ground state charge transfer complexes. As shown in Figure 6 for the methano-C<sub>60</sub> derivative V in room-temperature hexane, intensities at the first fluorescence band (716 nm) are quenched with increasing DEA concentrations, and the quenching is accompanied by increases in intensities at longer fluorescence wavelengths. The increases in fluorescence intensities at longer wavelengths with increasing DEA concentrations, which become more evident when the observed fluorescence spectra are normalized at the first fluorescence peak (Figure 6, inset), are due to the formation of an emissive fullerene–DEA exciplex. In room-temperature toluene, quenchings of the excited singlet states of the methano-C<sub>60</sub> derivatives by DEA also result in the formation of emissive fullerene–DEA exciplexes. Shown in Figure 7 are results for VI, as an example. However, in a more polar solvent environment of chloroform or hexane–acetone mixture, there are no exciplex emissions, while fluorescence intensities of the methano-C<sub>60</sub> derivatives are still quenched efficiently by DEA. Observed fluorescence spectral profiles become independent of DEA concentrations. Thus, the quenching of fluorescence intensities

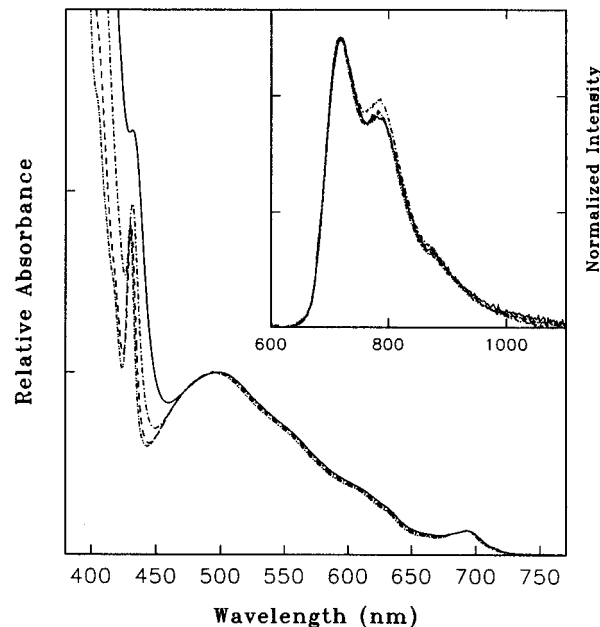


**Figure 3.** Absorption and fluorescence (inset) spectra of the methano-C<sub>60</sub> derivative II in toluene (···), *o*-xylene (---), 1,2,4-trimethylbenzene (— · —), and 1,2,3,5-tetramethylbenzene (—).

TABLE 2: Fluorescence Properties of the C<sub>60</sub> Derivatives

compound	solvent	$\Phi_F$ ( $10^{-3}$ )	$\tau_F$ (ns)	$k_{F,c}$ ( $10^5$ s <sup>-1</sup> )	$k_{F,c}$ ( $10^5$ s <sup>-1</sup> )
C <sub>60</sub>	toluene	0.32 <sup>a</sup>	1.2	2.7	4.8 <sup>a</sup>
I	toluene	1.07	1.51	7.1	4.8
II	toluene	1.14	1.49	7.65	4.9
III	toluene	1.19	1.47	8.1	5.1
IV	toluene	1.18	1.46	8.1	4.4
V	toluene		1.49		
VI	chloroform	1.05	1.48	7.1	4.2
VII	toluene	1.05	1.5	7.0	
	CH <sub>2</sub> Cl <sub>2</sub>	1.08			
	<i>o</i> -DCB	0.93			

<sup>a</sup> From ref 8.

in a more polar solvent environment may be evaluated in terms of the Stern–Volmer relationship.

$$\Phi_F^\circ/\Phi_F = 1 + k_q\tau_F^\circ[\text{DEA}] \quad (5)$$

where  $k_q$  is the quenching rate constant and  $\tau_F^\circ$  is the fluorescence lifetime in the absence of quencher. For the methano-C<sub>60</sub> derivative V in hexane with 10% (v/v) acetone, the Stern–Volmer plot (Figure 8) is not linear, exhibiting significant upward deviations at high DEA concentrations. The nonlinear Stern–Volmer behavior is most likely due to the contribution of static fluorescence quenching, which is more significant at high DEA concentrations.<sup>33</sup> In order to determine the quenching rate constant  $k_q$ , fluorescence quenchings were measured carefully at a series of low DEA concentrations ( $<0.05$  M). The Stern–Volmer plot of the results shown in

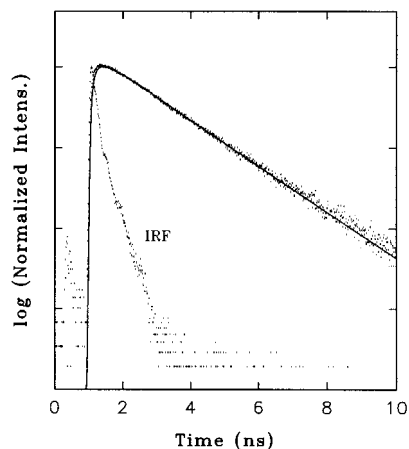


**Figure 4.** Fluorescence decay of the methano- $C_{60}$  derivative **I** in room-temperature toluene. The solid line is from a least-squares fit.

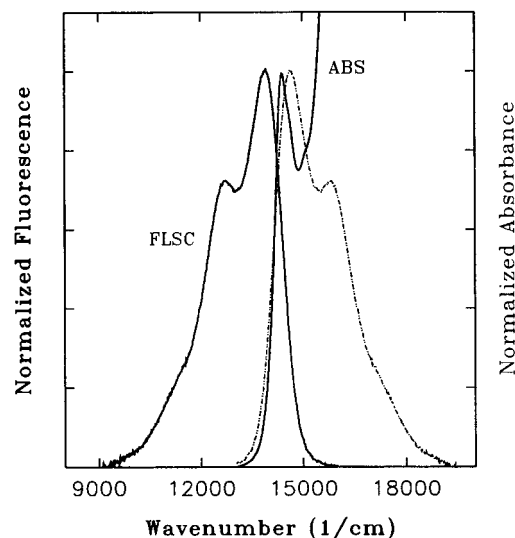


**Figure 5.** The assumed mirror image relationship for the calculation of the fluorescence radiative rate constant  $k_{F,c}$  of the methano- $C_{60}$  derivative **IV**.

Figure 8 (inset) is essentially linear. A least-squares regression yields a Stern–Volmer constant  $k_q\tau_F^\circ$  of  $28 \text{ M}^{-1}$ . With the known fluorescence lifetime  $\tau_F^\circ$  of 1.49 ns, the quenching rate constant  $k_q$  is  $1.9 \times 10^{10} \text{ M}^{-1} \text{ s}^{-1}$ .

The results shown in Figure 8 may be treated by use of an equation that takes into consideration static quenching contributions.<sup>33,34</sup>

$$\Phi_F^\circ/\Phi_F = (1 + k_q\tau_F^\circ[\text{DEA}]) \exp(N\nu[\text{DEA}]) \quad (6)$$

where  $N$  is Avogadro's number and  $\nu$  is the static quenching volume. With the known  $k_q$  and  $\tau_F^\circ$  values, a least-squares regression of the plot shown in Figure 8 yields the static quenching volume  $\nu$  of  $3022 \text{ \AA}^3$ . If the quenching volume is assumed to be spherical, the  $\nu$  value corresponds to a static fluorescence quenching radius of  $\sim 9 \text{ \AA}$  for the methano- $C_{60}$  derivative **V** in hexane with 10% (v/v) acetone, which is larger than the van der Waals radius of the  $C_{60}$  cage of  $\sim 5 \text{ \AA}$ .

The behavior of the pyrrolidino- $C_{60}$  derivative **VII** is apparently somewhat different. In saturated hydrocarbon solvents such as hexane and methylcyclohexane at room temperature, fluorescence intensities are not quenched by DEA at concentrations up to 0.3 M. At even higher DEA concentrations, changes in observed absorption spectra of **VII** due to the formation of ground state charge transfer complexes become evident. How-

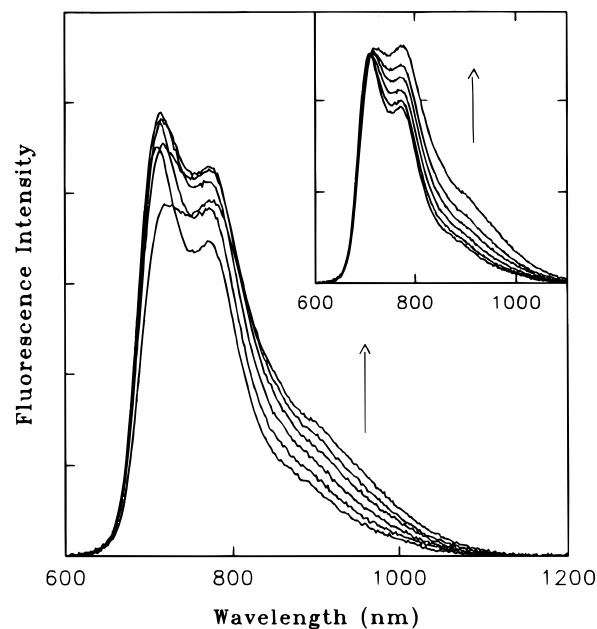


**Figure 6.** Observed fluorescence spectra of the methano- $C_{60}$  derivative **V** ( $\sim 2 \times 10^{-5} \text{ M}$ ) in room-temperature hexane at different DEA concentrations. The DEA concentrations are (in the direction of the arrow) 0, 0.036, 0.09, 0.15, 0.21, and 0.3 M. Shown in the inset are the spectra normalized at the first peak.

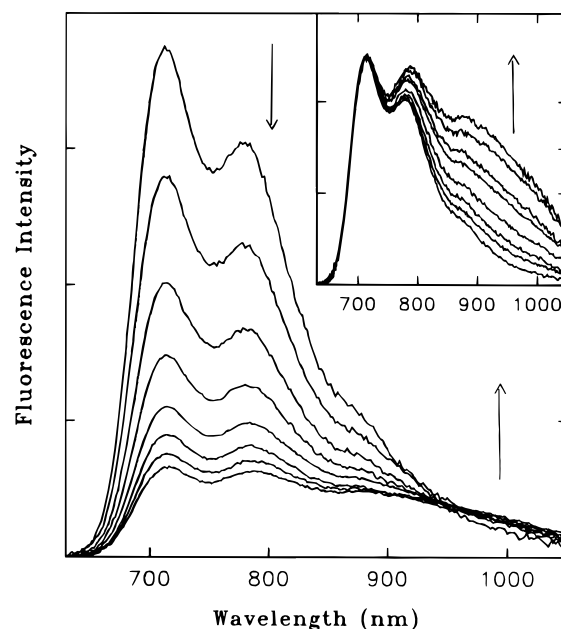


**Figure 7.** Observed fluorescence spectra of the methano- $C_{60}$  derivative **VI** ( $7 \times 10^{-6} \text{ M}$ ) in room-temperature toluene at different DEA concentrations. The DEA concentrations are (in the direction of the arrow) 0, 0.036, 0.09, 0.15, 0.21, and 0.3 M. Shown in the inset are the spectra normalized at the first peak.

ever, the quenching of fluorescence intensities of **VII** is significant in toluene or hexane with 10% (v/v) acetone at DEA concentrations similar to those for the methano- $C_{60}$  derivatives discussed above ( $< 0.3 \text{ M}$ ). In toluene, there is apparently the formation of an emissive **VII**–DEA exciplex (Figure 9).

## Discussion

The photophysical properties of the methano- and pyrrolidino- $C_{60}$  derivatives are in many ways similar to those of  $C_{60}$ . The overall increases in molar absorptivities of the derivatives may be attributed to a reduction in molecular symmetry due to the

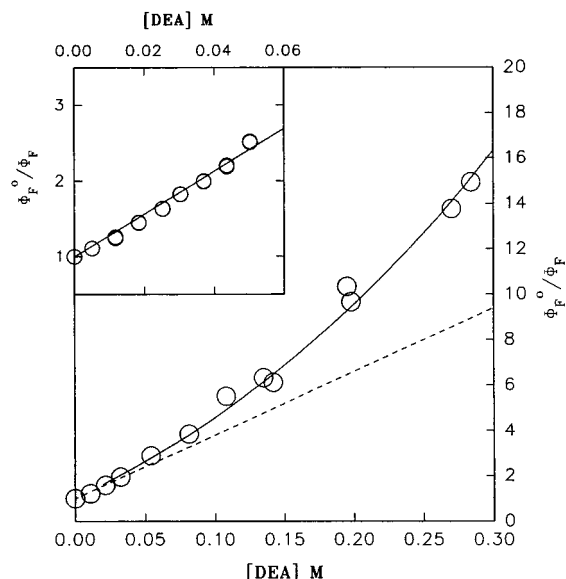


**Figure 8.** Fluorescence quenching ratios  $\Phi_F^0/\Phi_F$  for the methano- $C_{60}$  derivative **V** at different DEA concentrations in room-temperature hexane with 10% (v/v) acetone. The solid line is from eq 6, with the Stern–Volmer constant  $k_q\tau_F^0 = 28 \text{ M}^{-1}$  obtained from the results at low DEA concentrations shown in the inset and  $N\nu = 1.8$  obtained from a nonlinear least-squares regression.

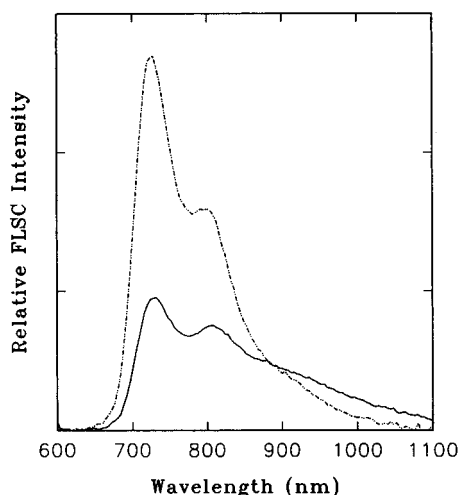


**Figure 9.** Observed fluorescence spectra of the pyrrolidino- $C_{60}$  derivative **VII** ( $6 \times 10^{-6} \text{ M}$ ) in room-temperature toluene (---) and with 0.3 M of DEA (—).

functionalization of the  $C_{60}$  cage. Interestingly, however, the absorption spectra and molar absorptivities of the methano- $C_{60}$  derivatives with different substituents are very similar, indicating that the transitions are dictated by the electronic structures of the functionalized fullerene moiety. For the pyrrolidino- $C_{60}$  derivative **VII**, the overall absorption spectrum is somewhat different from those of the methano- $C_{60}$  derivatives **I–VI**, but it also consists of a weak absorption band at  $\sim 700 \text{ nm}$  that is assigned to the 0–0 transition. It may thus be concluded on the basis of the absorption results that the lowest electronic transitions in the  $C_{60}$  derivatives have similar energies and transition probabilities. The conclusion is further supported by the fluorescence results. The fluorescence spectra, quantum yields, and lifetimes of the different  $C_{60}$  derivatives are all very similar. A common molecular structural feature in the methano- and pyrrolidino- $C_{60}$  derivatives under consideration is the 1,2-addition (6,6-closed) to the  $C_{60}$  cage. The similarities in the absorption and fluorescence properties of the two different

classes of  $C_{60}$  derivatives again suggest that the 0–0 transitions are dictated by the electronic structures of the 1,2-functionalized  $C_{60}$  cages.

The pyrrolidino- $C_{60}$  derivative **VII** is a linked fullerene–tertiary amine system, for which the possibility of excited state intramolecular electron transfer should be considered. However, the fluorescence quantum yield and lifetime of **VII** in toluene are very similar to those of the methano- $C_{60}$  derivatives (Table 2), suggesting no electron transfer quenching. The fluorescence quantum yields of **VII** in solvents of different polarities are similar, which is also against the possibility of intramolecular electron transfer quenching of the fullerene excited state. In fact, it is known<sup>35</sup> that the intermolecular electron transfer quenching of  $C_{60}$  fluorescence by triethylamine is strongly dependent on solvent polarity.

The methano- $C_{60}$  derivatives **I–VI** and the pyrrolidino- $C_{60}$  derivative **VII** all have a weak absorption band at  $\sim 700 \text{ nm}$  and rather similar fluorescence spectra. The results may be used as evidence for the argument that absorptions in the visible region (440–650 nm) are due primarily to contributions of electronic transitions other than the 0–0 transition. The absorption contributions in the region should therefore not be included in the calculation of fluorescence radiative rate constants by use of the Strickler–Berg equation. With the assumption that the absorption due to the lowest electronic transition may be estimated by the mirror image of the observed fluorescence spectrum, the calculated fluorescence radiative rate constants  $k_{F,c}$  of the  $C_{60}$  derivatives are smaller than the experimental  $k_{F,e}$  values obtained from fluorescence quantum yield and lifetime results (Table 2). For  $C_{60}$ , it has been shown<sup>8</sup> that a similar estimate of the lowest lying electronic transition probability with the assumed absorption–fluorescence mirror image relationship results in a  $k_{F,c}$  value larger than the  $k_{F,e}$  value. Nevertheless, because the calculation of  $k_{F,c}$  values is sensitive to the rough assumption of a mirror image relationship between fluorescence and absorption and also to other approximations associated with the Strickler–Berg equation,<sup>20</sup> some discrepancies between  $k_{F,c}$  and  $k_{F,e}$  values might be expected. A qualitative conclusion is that for  $C_{60}$  and the  $C_{60}$  derivatives in room-temperature solution the lowest energy absorption and the fluorescence are associated with the same excited singlet state.

Characteristic changes in observed absorption spectra of  $C_{60}$  and the  $C_{60}$  derivatives in the solvent series of methyl-substituted benzenes (Figure 3) are interesting. The absorption in the visible region (480–750 nm) is insensitive to solvent changes, while the intense second absorption band undergoes significant solvatochromic shifts. A simple explanation might be that the electronic transitions responsible for the visible absorption are only weakly allowed, essentially inert to solvent effects. Other systems exhibiting such properties include long-chain polyenes and diphenylpolyenes, which have been investigated extensively.<sup>36</sup> In the polyenes, the absorption spectra are due to strongly allowed electronic transitions ( ${}^1B_u^* \rightarrow {}^1A_g$ ) and undergo significant solvatochromic shifts, whereas the fluorescence spectra are due to weakly allowed transitions ( ${}^1A_g \leftarrow {}^1A_g^*$ ) and thus are hardly solvent dependent.<sup>36</sup> However, a special feature for the solvent dependence of the absorption spectra of  $C_{60}$  and the  $C_{60}$  derivatives is that it is very solvent specific. The nature of apparently specific interactions between the fullerene species and methyl-substituted benzenes remains an interesting question for further experimental and theoretical investigations.

Similar to  $C_{60}$ , the  $C_{60}$  derivatives are electron acceptors in both ground and excited states. Quenchings of the fluorescence intensities of  $C_{60}$  and the  $C_{60}$  derivatives by DEA apparently

share some common features.<sup>1b,32,33</sup> The electron transfer process between the excited singlet fullerene and DEA is inefficient in nonpolar saturated hydrocarbon solvents such as hexane and methylcyclohexane, so inefficient for the pyrrolidino-C<sub>60</sub> derivative **VII** that the fluorescence quenching is absent. A similar absence of fluorescence quenching in nonpolar saturated hydrocarbon solvents has been reported for the C<sub>60</sub>–triethylamine system.<sup>35</sup> In a more polar solvent environment with the presence of a polar cosolvent, quenches of the excited singlet states of the derivatives by DEA are not only close to diffusion-controlled but also consist of substantial contributions from static interactions (Figure 8).<sup>33</sup>

For the formation of exciplex, a difference between C<sub>60</sub> and the C<sub>60</sub> derivatives is that the C<sub>60</sub>–DEA exciplex emission can only be observed in nonpolar saturated hydrocarbon solvents, while for the C<sub>60</sub> derivatives there are also exciplex emissions in toluene, a solvent that is nonpolar but more polarizable than saturated hydrocarbons. However, despite the somewhat different solvent sensitivity for the exciplex emission, the fundamental excited state processes of C<sub>60</sub> and the C<sub>60</sub> derivatives in the presence of DEA should be similar. The absence of exciplex emissions in a more polar or polarizable solvent environment is likely due to solvent polarity effects. For the exciplex state, a competing decay process to fluorescence might be ionization for the formation of solvated ion pairs, which is strongly solvent polarity dependent.<sup>37</sup> In fact, the observation of radical cation and anion species in a transient absorption study of C<sub>60</sub>–amine systems in room-temperature toluene has been reported.<sup>38</sup>

**Acknowledgment.** We thank Bing Liu for experimental assistance and Dr. James Gord of the Wright Laboratory for the use of TCSPC equipment for some of the fluorescence lifetimes. Financial support from the National Science Foundation (CHE-9320558) is gratefully acknowledged. The research assistantships provided to B.M. and C.E.B. were provided in part by the Department of Energy through DOE/EPSCoR cooperative agreement DE-FG02-91ER75666.

## References and Notes

- (1) (a) Foote, C. S. In *Topics in Current Chemistry: Electron Transfer I*; Mattay, J., Ed.; Springer-Verlag: Berlin, 1994; p 347. (b) Sun, Y.-P. In *Molecular and Supramolecular Photochemistry, Vol. 1*; Ramamurthy, V., Ed.; Marcel Dekker: New York, 1997, in press.
- (2) (a) Ajie, H.; Alvarez, M. M.; Anz, S. J.; Beck, R. D.; Diederich, F.; Fostiropoulos, K.; Huffman, D. R.; Kratschmer, W.; Rubin, Y.; Schriver, K. E.; Sensharma, D.; Whetten, R. L. *J. Phys. Chem.* **1990**, *94*, 8630. (b) Taylor, R.; Hare, J. P.; Abdulsada, A.; Kroto, H. W. *J. Chem. Soc., Chem. Commun.* **1990**, 1423.
- (3) Arbogast, J. W.; Darmanyan, A. P.; Foote, C. S.; Rubin, Y.; Diederich, F. N.; Alvarez, M. M.; Whetten, R. B. *J. Phys. Chem.* **1991**, *95*, 11.
- (4) Sun, Y.-P.; Wang, P.; Hamilton, N. B. *J. Am. Chem. Soc.* **1993**, *115*, 6378.
- (5) Arbogast, J. W.; Foote, C. S. *J. Am. Chem. Soc.* **1991**, *113*, 8886.
- (6) Sun, Y.-P.; Bunker, C. E. *J. Phys. Chem.* **1993**, *97*, 6770.
- (7) (a) Wang, Y. *J. Phys. Chem.* **1992**, *96*, 764. (b) Sibley, S. P.; Argentine, S. M.; Francis, A. H. *Chem. Phys. Lett.* **1992**, *188*, 187. (c) Catalán, J.; Elguero, J. *J. Am. Chem. Soc.* **1993**, *115*, 9249.
- (8) Ma, B.; Sun, Y.-P. *J. Chem. Soc., Perkin Trans. 2* **1996**, 2157.
- (9) Isaacs, L.; Diederich, F. *Helv. Chim. Acta* **1993**, *76*, 2454.
- (10) Maggini, M.; Scorrano, G.; Prato, M. *J. Am. Chem. Soc.* **1993**, *115*, 9798.
- (11) Hirsch, A. *The Chemistry of Fullerenes*; Thieme: Stuttgart, 1994.
- (12) Diederich, F.; Thilgen, C. *Science* **1996**, *271*, 317.
- (13) (a) Friedman, S. H.; DeCamp, D. L.; Sijbesma, R. P.; Srdanov, G.; Wudl, F.; Kenyon, G. L. *J. Am. Chem. Soc.* **1993**, *115*, 6506. (b) Sijbesma, R.; Srdanov, G.; Wudl, F.; Castoro, J. A.; Wilkins, C.; Friedman, S. H.; De Camp, D. L.; Kenyon, G. L. *J. Am. Chem. Soc.* **1993**, *115*, 6510.
- (14) Toniolo, C.; Bianco, A.; Maggini, M.; Scorrano, G.; Prato, M.; Marastoni, M.; Tomatis, R.; Spisani, S.; Palù, G.; Blair, E. D. *J. Med. Chem.* **1994**, *37*, 4558.
- (15) (a) Foote, C. S. *ACS Symp. Ser. 616 (Light Activated Pest Control)* **1995**, *17*. (b) Jensen, A. W.; Wilson, S. R.; Schuster, D. I. *Bioorg. Med. Chem.* **1996**, *4*, 767.
- (16) (a) Signorini, R.; Zerbetto, M.; Meneghetti, M.; Bozio, R.; Maggini, M.; De Faveri, C.; Prato, M.; Scorrano, G. *J. Chem. Soc., Chem. Commun.* **1996**, 1891. (b) Maggini, M.; Scorrano, G.; Prato, M.; Brusatin, G.; Innocenzi, P.; Guglielmi, M.; Renier, A.; Signorini, R.; Meneghetti, M.; Bozio, R. *Adv. Mater.* **1995**, *7*, 404. (c) Cha, M.; Sariciftci, N. S.; Heeger, A. J.; Hummelen, J. C.; Wudl, F. *Appl. Phys. Lett.* **1993**, *67*, 3850.
- (17) Sun, Y.-P.; Riggs, E. J.; Liu, B. *Chem. Mat.* **1997**, *9*, 1268.
- (18) (a) Anderson, J. L.; An, Y.-Z.; Rubin, Y.; Foote, C. S. *J. Am. Chem. Soc.* **1994**, *116*, 9763. (b) Lin, S.-K.; Shiu, L.-L.; Chien, K. M.; Luh, T.-Y.; Lin, T.-I. *J. Phys. Chem.* **1995**, *99*, 105. (c) Guldi, D. M.; Asmus, K.-D. *J. Phys. Chem.* **1997**, *101*, 1472.
- (19) Sun, Y.-P.; Ma, B.; Riggs, J. E.; Bunker, C. E. In *Fullerenes, Recent Advances in the Chemistry and Physics of Fullerenes and Related Materials, Vol. 4*; Kadish, K. M.; Ruoff, R. S., Eds.; The Electrochemical Society Inc.: Pennington, NJ, in press.
- (20) Strickler, S. J.; Berg, R. A. *J. Chem. Phys.* **1962**, *37*, 814.
- (21) Sension, R. J.; Phillips, C. M.; Szarka, A. Z.; Romanow, W. J.; McGhie, A. R.; McCauley, J. P., Jr.; Smith, A. B., III; Hochstrasser, R. M. *J. Phys. Chem.* **1991**, *69*, 6075.
- (22) Kim, D.; Lee, M.; Suh, Y. D.; Kim, S. K. *J. Am. Chem. Soc.* **1992**, *114*, 4429.
- (23) Wang, Y.; Cao, J.; Schuster, D. I.; Wilson, S. R. *Tetrahedron Lett.* **1995**, *36*, 6843.
- (24) Bingel, C. *Chem. Ber.* **1993**, *126*, 1957.
- (25) Lawson, G. E.; Kitaygorodskiy, A.; Ma, B.; Bunker, C. E.; Sun, Y.-P. *J. Chem. Soc., Chem. Commun.* **1995**, 2225.
- (26) Bunker, C. E.; Sun, Y.-P.; Gord, J. R. *J. Am. Chem. Soc.*, submitted.
- (27) Isaacs, L.; Diederich, F. *Helv. Chim. Acta* **1993**, *76*, 1231.
- (28) Catalán, J.; Saiz, J. L.; Laynez, J. L.; Jagerovic, N.; Elguero, J. *Angew. Chem., Int. Ed. Engl.* **1995**, *34*, 105.
- (29) Karstens, T.; Kobs, K. *J. Phys. Chem.* **1980**, *84*, 14.
- (30) For **VI**, the decay consists of minor contribution from a short-lived component, which might be attributed to scattering or trace amount of impurity.
- (31) Williams, R. M.; Zwier, J. M.; Verhoeven, J. W. *J. Am. Chem. Soc.* **1995**, *117*, 4093.
- (32) Palit, D. K.; Ghosh, H. N.; Pal, H.; Sapre, A. V.; Mittal, J. P.; Seshadri, R.; Rao, C. N. R. *Chem. Phys. Lett.* **1992**, *198*, 113.
- (33) Sun, Y.-P.; Bunker, C. E.; Ma, B. *J. Am. Chem. Soc.* **1994**, *116*, 9692.
- (34) Birks, J. B. *Photophysics of Aromatic Molecules*; Wiley-Interscience: London, 1970.
- (35) Sun, Y.-P.; Ma, B.; Lawson, G. E. *Chem. Phys. Lett.* **1995**, *233*, 57.
- (36) (a) Hudson, B. S.; Kohler, B. E.; Schulten, K. In *Excited States*; Lim, E. C., Ed.; Academic Press: New York, 1982; Vol. 6, p 1. (b) Saltiel, J.; Sun, Y.-P. In *Photochromism, Molecules and Systems*; Dürr, H.; Bouas-Laurent, H., Eds.; Elsevier: Amsterdam, 1990; p 64. (c) Kohler, B. E. *Chem. Rev.* **1993**, *93*, 41.
- (37) Sun, Y.-P.; Ma, B. *Chem. Phys. Lett.* **1995**, *236*, 285.
- (38) (a) Ghosh, H. N.; Pal, H.; Sapre, A. V.; Mittal, J. P. *J. Am. Chem. Soc.* **1993**, *115*, 11722. (b) Park, J.; Kim, D.; Suh, Y. D.; Kim, S. K. *J. Phys. Chem.* **1994**, *98*, 12715. (c) Ito, O.; Sasaki, Y.; Yoshikawa, Y.; Watanabe, A. *J. Phys. Chem.* **1995**, *99*, 9838. (d) Sasaki, Y.; Yoshikawa, Y.; Watanabe, A.; Ito, O. *J. Chem. Soc., Faraday Trans.* **1995**, *91*, 2287.